Journal of Nanoscience and Nanotechnology
Vol. 12, 6065–6068, 2012

RESEARCH ARTICLE

Fabrication and Photovoltaic Properties of Heterostructured TiO_2 Nanowires

Suk-In Noh[1], Dong-Won Park[2], Hee-Sang Shim[2,*], and Hyo-Jin Ahn[1,*]

[1] *Department of Materials Science and Engineering, Seoul National University of Science and Technology, Seoul 139-743, South Korea*
[2] *Research Institute for Solar and Sustainable Energies (RISE), Gwangju Institute of Science and Technology (GIST), Gwangju 500-712, South Korea*

One-dimensional heterostructured TiO_2 nanowires were successfully fabricated by an electrospinning technique and modified by hydrolysis. We investigated their structure, morphology, chemical composition, and optical properties by using the X-ray diffraction (XRD), scanning electron microscopy (SEM), transmission electron microscopy (TEM), X-ray photoelectron spectroscopy (XPS), and UV-vis spectroscopy. In the case of the photovoltaic performance, the short-circuit current density and cell efficiency of the DSSCs employing single TiO_2 nanowires and heterostructured TiO_2 nanowires improve from 6.90 to 11.38 mA/cm^2 and from 2.56 to 4.29%, respectively. The results show that the photoconversion efficiency of the heterostructured TiO_2 nanowires could be improved by more than ~67% compared to that of the single TiO_2 nanowires because of the enhanced specific surface area that facilitates dye adsorption.

Keywords: TiO_2, Heterostructured Nanowires, Electrospinning, Photovoltaic Properties.

1. INTRODUCTION

Dye-sensitized solar cells (DSSCs) are presently receiving significant attention as potential alternatives to conventional crystalline solar cells because of their high conversion efficiency and low manufacturing cost.[1] A DSSC consists of an *n*-type semiconductor electrode such as TiO_2 and ZnO with a solar-energy absorbing dye, an electrolyte, and a counter electrode; the cell is a photovoltaic device based on the principles of plant photosynthesis.[1–3]

Titanium dioxide (TiO_2) is an *n*-type semiconductor that has wide applications as a photocatalyst, catalyst support, dielectric material, photovoltaic electrode, and pigment materials.[3–5] In particular, among the various applications, TiO_2 has been widely used as photoelectrodes in photovoltaic cells such as DSSCs. Considerable effort has been devoted to improve the performance of DSSCs via various synthetic methods such as sol–gel, hydrolysis, hydro-/solve-thermal, anodizing, vacuum deposition, sonochemical, and microwave-assisted methods. In addition, one-dimensional TiO_2 nanostructures have been actively studied because of their unusual and unique characteristics.[4–7] For example, Kang et al. reported the fabrication of highly ordered TiO_2 nanotubes with an efficiency of 3.5% using a nanoporous alumina templating method.[8] Moreover, Feng et al. presented tantalum-doped TiO_2 nanowire arrays hydrothermally synthesized for DSSCs with a conversion efficiency of 4.1%.[9] Oh et al. argued that TiO_2-branched nanostructure electrodes that were fabricated by a seeding method had a conversion efficiency of 4.3%.[10] The study of the use of one-dimensional nanostructures in DSSCs is underway, and the relation between the one-dimensional nanostructures and the photovoltaic performances has not been clearly understood hitherto.

In this study, heterostructured TiO_2 nanowire (NW) electrodes, consisting of TiO_2 nanoparticles decorated on TiO_2 nanowires, were successfully fabricated by means of an electrospinning method with a hydrolysis reaction. Subsequently, their structural properties and photovoltaic performances of DSSCs were investigated.

2. EXPERIMENTAL DETAILS

TiO_2 NWs were synthesized using an electrospinning method. In the electrospinning process, titanium tetraisopropoxide (Ti(O*i*Pr)$_4$, Aldrich) was mixed with anhydrous ethanol and acetic acid. After stirring for 10 min, the solution was mixed with the polymer carrier solution of poly(vinylpyrrolidone) (PVP, $M_w = 1{,}300{,}000$ g/mol,

*Authors to whom correspondence should be addressed.

Aldrich) dissolved in ethanol, and then stirred for 30 min. Then, the blended solution was placed in a syringe with a 23-gauge stainless steel needle. The feeding rate and the tip-to-collector distance were controlled to be ~0.04 ml/h and ~8 cm, respectively, under an applied voltage of 8 kV during electrospinning. Single TiO_2 nanowires were obtained by removing PVP from the as-spun nanowires via calcination at 500 °C for 5 h in air. In order to fabricate the heterostructured TiO_2 nanowires, electro-spun TiO_2 nanowires were dispersed in DI water, which was added to a precursor of $Ti(O\textit{i}Pr)_4$ mixed with 2-propanol solution. After hydrolysis for 6 h at room temperature, the heterostructured TiO_2 nanowires were washed by DI water. Then, heterostructured TiO_2 nanowires were successfully obtained by freeze-drying at −50 °C. For the assembly of DSSCs, fluorine-doped tin oxide coated glasses (FTO, 15 Ω/cm^2, Solaronix) were ultrasonically cleaned by acetone, methanol, ethanol, and DI water. The DSSCs consisted of a working electrode, a counter electrode, and an electrolyte, respectively. For the fabrication of the working electrodes, a TiO_2 paste was prepared by using 16.2 wt% of single/heterostructured TiO_2 nanowires, 11.9 wt% of hydroxypropyl cellulose (HPC, $M_w \sim 80{,}000$ g/mol, Aldrich), 4.4 wt% of acetyl acetone (Aldrich), and 67.5 wt% of DI water. The mixture was ground in an agate mortar for 6 h to obtain a viscous paste. Subsequently, the single/heterostructured TiO_2 films were fabricated by coating the prepared TiO_2 paste on the cleaned FTO glass using a squeeze printing technique and then sintering at 500 °C for 1 h. The calcined TiO_2 electrodes were immersed in 0.5 mM $Ru(dcbpy)_2(NCS)_2$ (535-bis TBA, Solaronix) and dissolved in ethanol overnight (~24 h). The Pt-coated FTO glass counter electrode was prepared by coating with platinum paste (PT-1, Dyesol) and sequential sintering at 450 °C for 30 min. The prepared working and counter electrodes were assembled into a sandwich, and filled with a 0.3 M DMPII based electrolyte.[11] The structural properties of the heterostructured TiO_2 NWs were established by X-ray diffraction (XRD, Rigaku X-ray diffractormeter equipped with a Cu Kα radiation), scanning electron microscopy (SEM, Hitachi S-4700), and high-resolution electron microscopy (HREM, JEOL, 2100F, KBSI Suncheon center) analyses. The chemical bonding states of the samples were examined using X-ray photoelectron spectroscopy (XPS, ESCALAB 250 equipped with an Al Kα X-ray source). The optical properties of the samples were investigated by using UV-vis spectrometer (Jasco V650). The photovoltaic properties of the DSSCs were evaluated by using a 150 W xenon lamp (LAB 50) with the standard irradiance level (100 mW cm^{-2}) for the active sample areas of 0.196 cm^2.

3. RESULTS AND DISCUSSION

We used X-ray diffraction (XRD) to investigate the structural properties of the single TiO_2 NWs and the heterostructured TiO_2 NWs, as shown in Figure 1. The single TiO_2 NWs are well-crystallized via calcination at 500 °C, as indicated by the sharp diffraction peaks for the anatase/rutile mixed structure. The characteristic diffraction peaks at 25.3°, 37.8°, 48.0°, 53.9°, 62.7°, and 68.8° correspond to the (101), (004), (200), (105), (204), and (116) planes, respectively, of anatase TiO_2 (JCPDS No. 841286). In addition, the peaks at 27.9°, 36.4°, 41.7°, and 55.1° correspond to the (110), (101), (111), and (211) planes of rutile TiO_2 (JCPDS No. 881175). For the characteristic peaks of the single TiO_2 NWs, the phase composition of the TiO_2 nanocomposite can be estimated according to the equation below:

$$W_R = A_R/(0.884 \cdot A_A + A_R)$$

where W_R, A_A, and A_R are the weight percentage of the rutile structure, the integrated intensity of the (101) anatase peak, and the integrated intensity of the (110) rutile peak, respectively.[12] The rutile weight percentage in the single TiO_2 NWs was estimated to be ~27.4%, whereas the heterostructured TiO_2 NWs have a relatively anatase-rich crystal structure with ~22% rutile content compared to the single TiO_2 NWs. This result indicates that the increase of anatase content on the NW surface may be attributed to the NW modification via the hydrolysis reaction in titanium

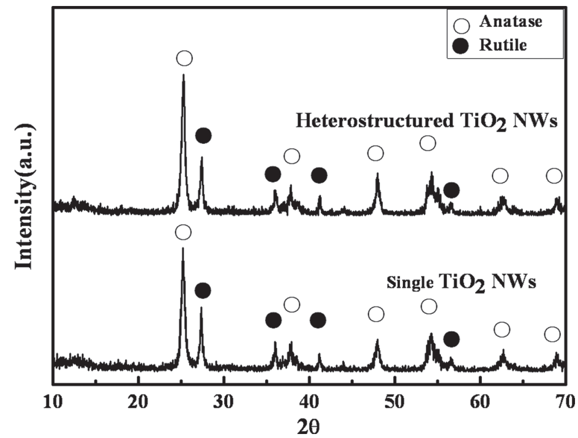

Fig. 1. XRD plots of the single TiO_2 nanowires and the heterostructured TiO_2 nanowires.

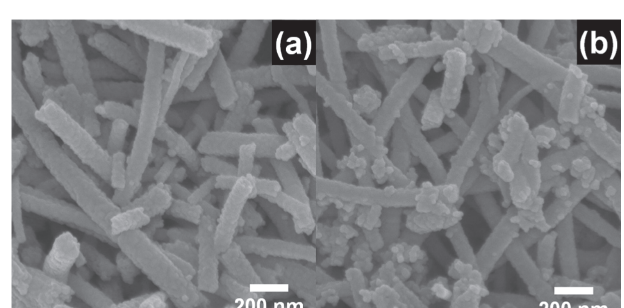

Fig. 2. SEM images of (a) the single TiO_2 nanowires and (b) the heterostructured TiO_2 nanowires.

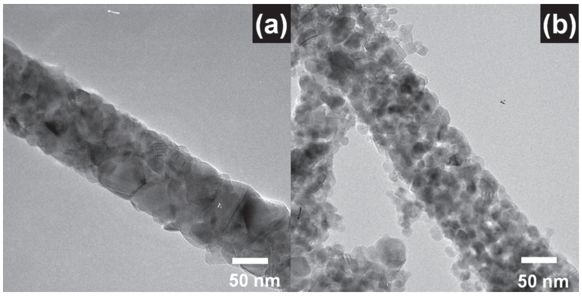

Fig. 3. HRTEM images obtained from (a) the single TiO_2 nanowires and (b) the heterostructured TiO_2 nanowires.

tetraisopropoxide (TTIP) solution. It has been known that anatase TiO_2-based solar cells exhibit better photoelectrochemical performances compared to rutile TiO_2-based solar cells owing to the large surface area that facilitates dye adsorption. This property can be easily confirmed from the photocurrent density–voltage curves.[13]

Figure 2 shows SEM images of the single TiO_2 NWs and the heterostructured TiO_2 NWs. The single TiO_2 NWs have a smooth surface with a diameter of ~80–130 nm after calcination at 500 °C, and the nanoparticles that formed on the nanowire surface of the heterostructured TiO_2 NWs via the hydrolysis of the TTIP precursor as reported elsewhere[14, 15] had formed with the size of several nm. The rutile/anatase ratio change mentioned in Figure 1 is probably caused by the formation of such a second phase. However, the diameter of the support nanowires remained the same as that of the single NWs after the TTIP treatment, and the nanoparticles were randomly distributed on the TiO_2 NW surface, which may increase the number of adsorption sites for dye molecules.

Figure 3 shows the HRTEM images obtained from the single and the heterostructured TiO_2 NWs. The single TiO_2 NW shows a dense crystal structure with a diameter of ~100 nm after calcination at 500 °C. However, the heterostructured TiO_2 NW obtained by post TTIP treatment of electro-spun TiO_2 NW seems to consist of crystalline nanoparticles with a size of 5–10 nm covering the dense NW surface. In other words, smaller grains form on

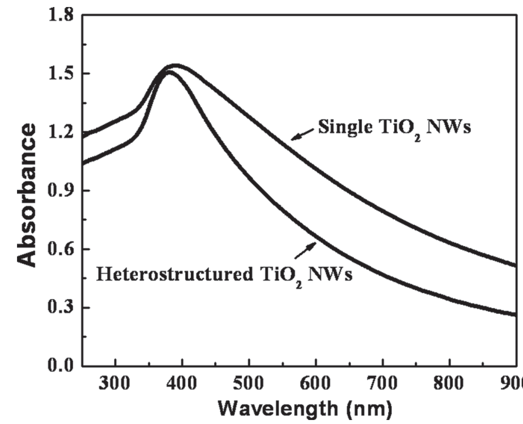

Fig. 5. UV-vis absorption spectra of the single TiO_2 nanowires and the heterostructured TiO_2 nanowires.

the heterostructured TiO_2 NWs relative to the single TiO_2 NWs. The heterostructure formation of the nanoparticles on NWs should contribute to an increase in the surface area. Therefore, such morphology modification of the TiO_2 NW surface will affect photovoltaic characteristics such as photocurrent density and conversion efficiency.

We conducted XPS measurements to examine the chemical bonding state of the samples. The photoelectron energies of the Ti $2p$ peaks were corrected by considering the reference C $1s$ peak at 284.5 eV. Figures 4(a) and (b) show the XPS core-level spectra for the Ti $2p_{3/2}$ and Ti $2p_{1/2}$ photoelectrons with binding energies of ~458.5 eV and ~464.2 eV for the single TiO_2 NWs and the heterostructured TiO_2 NWs, respectively. The characteristic peaks of the heterostructured TiO_2 NWs exhibit no noticeable difference relative to those of the single TiO_2 NWs. This implies that the elemental Ti in TiO_2 is not Ti(II) species but Ti(IV) species.[16]

Figure 5 displays the UV-vis absorption spectra for the single TiO_2 NWs and the heterostructured TiO_2 NWs. The TTIP treatment obviously affects light absorption characteristics of TiO_2 NWs as shown in Figure 5. Generally, the main absorption of pure anatase TiO_2 appears at wavelengths shorter than 400 nm, which corresponds to

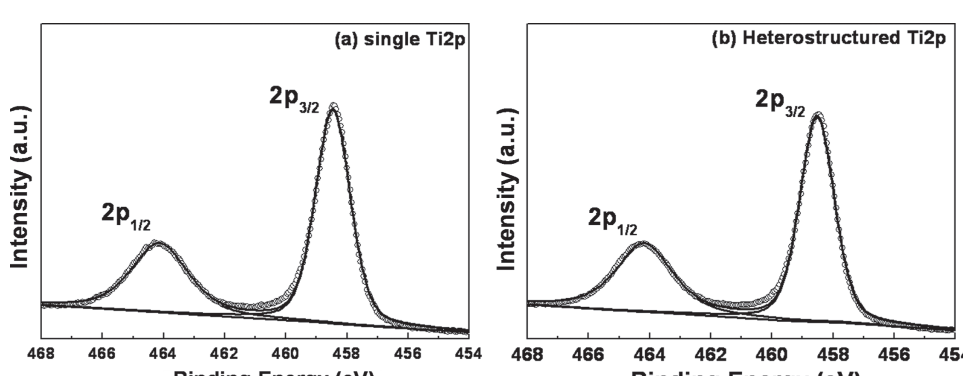

Fig. 4. XPS core-level spectra of the Ti $2p$ photoelectrons for (a) the single TiO_2 nanowires and (b) the heterostructured TiO_2 nanowires.

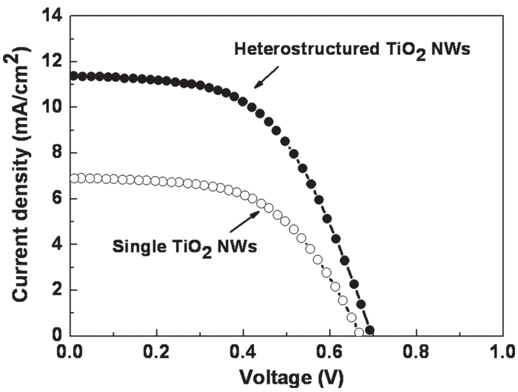

Fig. 6. Photocurrent density–voltage curves measured from the DSSCs using the single TiO_2 nanowires and the heterostructured TiO_2 nanowires.

Table I. Photovoltaic performances of DSSCs employing the single TiO_2 NWs and heterostructured TiO_2 NWs.

Samples	J_{sc} (mA/cm^2)	V_{oc} (V)	FF	η (%)
Heterostructured TiO_2 NWs	11.38	0.69	0.54	4.29
Single TiO_2 NWs	6.90	0.67	0.55	2.56

its intrinsic bandgap of 3.2 eV.[17] The maximum absorption peak and the absorption edge of the heterostructured TiO_2 NWs show a blue shift (ca.10 nm) in the bandgap transition compared to those of the single TiO_2 NWs. That is, the optical bandgap of the heterostructured TiO_2 NWs becomes larger slightly than that of the single TiO_2 NWs. This implies that the heterostructured TiO_2 NWs are anatase-rich phases. This result is good agreement with XRD results as shown in Figure 1.

Two different types of TiO_2 NWs were used as the photoanode in the dye-sensitized solar cells (DSSCs). The photocurrent density (J)–voltage (V) curves of the DSSCs assembled with single and heterostructured TiO_2 NWs are presented in Figure 6 and the derived DSSC curve parameters are summarized in Table I. For the case of DSSCs fabricated with single and heterostructured TiO_2 NWs, the V_{oc} changes are negligible. However, the DSSC fabricated with heterostructured TiO_2 NWs exhibits superior photovoltaic efficiency with enhanced photocurrent density compared to the DSSC fabricated with single TiO_2 NWs. In particular, the photoconversion efficiency (PCE; η) of DSSCs with single TiO_2 NWs and heterostructured TiO_2 NWs increases significantly from 2.56% to 4.29%. This implies that the PCE of the heterostructured TiO_2 NWs is $\sim$67% greater than that of the single TiO_2 NWs. This result indicates that the higher PCE can be attributed to the improvement of the photocurrent density resulting from an enhanced specific surface area. Therefore, the morphology modification of such one-dimensional heterostructure by the hydrolysis reaction in TTIP solution may significantly enhance the photoconversion efficiency of one-dimensional TiO_2 photoelectrodes rendering them useful for DSSCs.

4. SUMMARY

We synthesized heterostructured TiO_2 NWs by nanoparticle formation via hydrolysis of the TTIP precursor solution on electro-spun TiO_2 NWs for DSSCs. SEM and TEM images showed that after calcination, the surface morphology of the TTIP-treated TiO_2 NWs becomes rougher surface than that of single TiO_2 NWs. The DSSC device with the surface-modified TiO_2 heterostructure also shows higher photovoltaic performance because of the enhancement of the photocurrent density as well as the improvement of light absorption via higher dye loading.

Acknowledgments: This research was supported by Basic Science Research Program through the National Research Foundation of Korea (NRF) funded by the Ministry of Education, Science and Technology (2011-0005561) and the research subsidy of Seoul National University of Science and Technology for year 2012.

References and Notes

1. M. Grätzel, *Nature* 414, 338 (**2001**).
2. A. Umar, A. A. Alharbi, P. Singh, and S. A. Al-Sayari, *J. Nanosci. Nanotechnol.* 11, 3560 (**2011**).
3. D.-W. Park, K.-H. Park, J.-W. Lee, K.-J. Hwang, and Y.-K. Choi, *J. Nanosci. Nanotechnol.* 7, 3722 (**2007**).
4. S. Barth, F. Hernandez-Ramirez, J. D. Holmes, and A. Romano-Rodriguez, *Prog. Mater. Sci.* 55, 563 (**2010**).
5. H.-S. Shim, S.-I. Na, S. H. Nam, H.-J. Ahn, H. J. Kim, D.-Y. Kim, and W. B. Kim, *Appl. Phys. Lett.* 92, 183107 (**2008**).
6. L. Sun, S. Zhang, X. Sun, and X. He, *J. Nanosci. Nanotechnol.* 10, 4451 (**2010**).
7. J. Miao, M. Miyauchi, T. J. Simmons, J. S. Dordick, and R. J. Linhardt, *J. Nanosci. Nanotechnol.* 10, 5507 (**2010**).
8. T.-S. Kang, A. P. Smith, B. E. Taylor, and M. F. Durstock, *Nano Lett.* 9, 601 (**2009**).
9. J. Oh, J. Lee, H. Kim, S. Han, and K. Park, *Chem. Mater.* 22, 1114 (**2010**).
10. X. Feng, K. Shankar, M. Paulose, and C. Grimes, *Angewandte Chemie* 48, 8095 (**2009**).
11. H.-S. Lee, S.-H. Bae, Y. Jo, K.-J. Kim, Y. Jun, and C.-H. Han, *Electrochim. Acta* 55, 7159 (**2010**).
12. G. Li, C. P. Richter, R. L. Milot, L. Cai, C. S. Schmuttenmaer, R. H. Crabtree, G. W. Brudvig, and V. S. Batista, *Dalton Transactions* 10078 (**2009**).
13. N.-G. Park, J. van de Lagemaat, and A. J. Frank, *J. Phys. Chem. B* 104, 8989 (**2000**).
14. C. J. Barbe, F. Arendse, P. Comte, M. Jirousek, F. Lenzmann, V. Shklover, and M. Gratzel, *Journal of American Ceramic Society* 80, 3157 (**1997**).
15. Y. Hong, D. Li, J. Zheng, and G. Zou, *Nanotechnology* 17, 1986 (**2006**).
16. J. F. Moulder, W. F. Stickle, P. E. Sobol, and K. D. Bomben, *Physical Electronics, Eden Pairie, Physical Electronics Inc.* 1995, 72 (**1995**).
17. J. Yu, J. Yu, W. Ho, Z. Jiang, and L. Zhang, *Chem. Mater.* 14, 3808 (**2002**).

Received: 19 July 2011. Accepted: 30 January 2012.